

Title: Colonial Architecture Modulates the Speed and Efficiency of Multi-Jet Swimming in Salp Colonies

Authors: Alejandro Damian-Serrano¹, Kai A. Walton¹, Anneliese Bishop-Perdue¹, Sophie Bagoye¹, Kevin T. Du Clos², Bradford J. Gemmell³, Sean P. Colin^{4,5}, John H. Costello⁶, Kelly R. Sutherland¹

Author Affiliations:

(1) Institute of Ecology and Evolution, Department of Biology, University of Oregon. 473 Onyx Bridge, 5289 University of Oregon, Eugene, OR 97403-5289, USA.

(2) Louisiana Universities Marine Consortium, 8124 Highway 56, Chauvin, LA 70344, USA.

(3) Department of Integrative Biology, University of South Florida, 4202 East Fowler Avenue, Tampa, FL 33620, USA.

(4) Marine Biology and Environmental Science, Roger Williams University, Bristol, RI 02809, USA.

(5) Whitman Center, Marine Biological Laboratory, Woods Hole, MA 02543, USA.

(6) Biology Department, Providence College, Providence, RI 02918, USA.

Running title: Architecture Modulates Salp Swimming

Summary Statement (30 words)

Linear arrangements in multi-jet propelled marine colonial invertebrates are faster than less streamlined architectures without incurring in higher costs of transport, offering insights for bioinspired underwater vehicle design.

Abstract

Salps are marine pelagic tunicates with a complex life cycle including a solitary and colonial stage. Salp colonies are composed of asexually budded individuals that coordinate their swimming by multi-jet propulsion. Colonies develop into species-specific architectures with distinct zooid orientations. These distinct colonial architectures vary in how frontal area scales with the number of zooids in the colony. Based on findings from other jet-propelled systems, we hypothesize that differences in frontal area drive differences in swimming speed and that increased swimming speed leads to higher cost of transport in salps. We (1) compare swimming speed across salp species and architectures, (2) evaluate how swimming speed scales with the number of zooids across colony in architectures, and (3) compare the metabolic cost of transport across species and how it scales with swimming speed. To measure swimming speeds, we recorded swimming salp colonies using in situ videography while SCUBA diving in the open ocean. To estimate the cost of transport, we measured the respiration rates of swimming and anesthetized salps collected in situ using jars equipped with non-invasive oxygen sensors. We found that linear colonies generally swim faster due to their differential advantage in frontal area scaling with an increasing number of zooids. We also found that higher swimming speeds predict lower costs of transport in salps. These findings underscore the importance of considering propeller arrangement to optimize speed and energy efficiency in bioinspired underwater vehicle design, leveraging lessons learned from the diverse natural laboratory provided by salp diversity.

Keywords: salps, colonial architecture, multi-jet propulsion, swimming, cost of transport

Introduction

Salps (Tunicata: Thaliacea: Salpida) are planktonic invertebrates that have a two-phase life cycle comprised of a solitary oozoid that asexually buds colonies of sexually reproducing blastozooids. Salp colonies are composed of up to hundreds of genetically identical, physically and neurophysiologically integrated pulsatile zooids (Bone et al. 1980, Mackie 1986). Zooids in the colony feed and propel themselves by inhaling water through the oral siphon, using muscle contraction to compress their pharyngeal chamber, and exhaling a jet of water from their atrial siphon (Bone & Trueman 1983). While solitary oozoids move using single-jet propulsion, salp blastozooid colonies integrate multiple propelling jets, which increases their thrust and reduces

the drag that results from periodical acceleration and deceleration via asynchronous swimming (Sutherland & Weihs 2017).

Currently, there are 48 described species of salps (WoRMS, 2024) and differences between species have mainly been compared from a taxonomic lens, focused on zooid-level diagnostic morphological characters. While salps are widely distributed, most salp species are restricted to open ocean environments, far from the coast with extremely deep bottom depths, which poses unique challenges to accessing them for direct study in their environment (Hamner et al 1975, Haddock 2004). Moreover, salps cannot be maintained alive in containers beyond a few hours since they are extremely fragile and sensitive to the presence of solid walls. Therefore, many morphological, ecological, and functional aspects of salp diversity, such as swimming speeds and metabolic demands, have remained unexplored. One such aspect is colonial architecture or the way that the zooids are arranged relative to each other in the colony. Salp colonies develop into species-specific architectures with distinct zooid orientations, including transversal, oblique, linear, helical, and bipinnate chains; as well as whorls, and clusters (Damian-Serrano & Sutherland, 2023). These architectures present distinct orientations of the propeller zooids and their thrusting jets to the axes of colony elongation and locomotion hypothesized to have an impact on their swimming performance (Madin 1990, Damian-Serrano et al. 2023).

Linear salp chains have been hypothesized to be more efficient swimmers due to the reduction of drag associated with a more streamlined form (Bone & Trueman 1983). We expect frontal (pressure and form) drag scaling to be one of the relevant factors to the hydrodynamics of swimming salp colonies given that their intermediate Reynolds numbers are estimated to be between ~ 100 (Sutherland & Madin 2010) for solitary salps and ~ 5000 for linear chains (Sutherland & Weihs 2017). In animals swimming at high Reynolds numbers, such as colonial salps, the pressure drag experienced during swimming is expected to largely depend on the frontal (motion-orthogonal) projected area (Alexander 1968, Vogel 1981). In a multi-jet system, having a larger number of propellers is expected to improve the hydrodynamic and inertial benefits granted by asynchronous multijet propulsion, in addition to providing additional thrust to the colony (Madin 1990, Sutherland & Weihs 2017). The effect of varying numbers of propeller zooids on swimming speed has never been investigated in salps, nor how this relationship may vary across their diverse colonial architectures. While relative (per propeller unit) frontal area is greatly reduced in linear chains when compared to the sum of each separate blastozooid (Mackie 1986, Sutherland & Weihs 2017), we hypothesize that this advantage will be lower in species with non-linear colonial architectures, and thus we predict finding differences in swimming speed between colonial architectures. Salp colonial architectures differ in how the number of zooids in the colony

scales with their frontal area relative to motion (Madin 1990). Some architectures (linear, bipinnate, and helical) have a constant frontal area, regardless of zooid number. We expect these architectures to benefit from increased thrust delivered by larger numbers of zooids while maintaining a constant frontal area. However, the rest of the architectures (oblique, transversal, whorl, and cluster) have an increasing (directly proportional) frontal area as the number of zooids increases (Fig. 1). Therefore, we expect the latter architectures to not only obtain more thrust, but to also experience more frontal water resistance as a result of bearing a greater number of propeller zooids. As a result, we also predict that swimming speed will be greater in colonies that bear a larger number of zooids, but only (or more so) for species with architectures that have a constant frontal area.

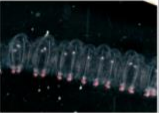
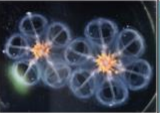





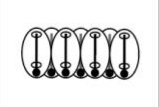
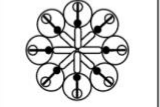



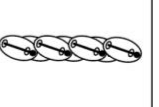

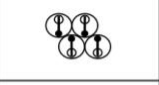
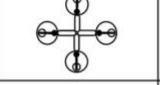
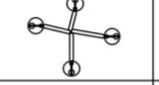
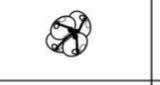
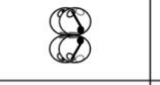
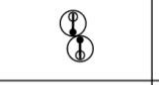
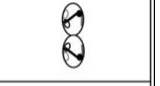
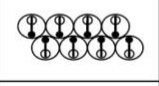
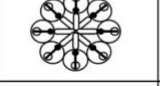
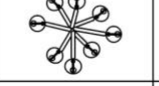

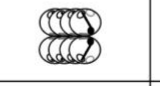
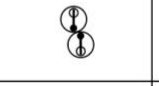
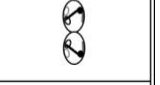
	Transversal	Whorl	Cluster	Helical	Oblique	Linear	Bipinnate
Architecture							
							
Frontal area 4 zooids							
Frontal area 8 zooids							
Scaling	2	2	2	1	$1 < x < 2$	1	1

Figure 1. Salp colonial architectures with representative species photos (*Pegea* sp. for transversal, *Cyclosalpa affinis* for whorl, *Cyclosalpa sewelli* for cluster, *Helicosalpa virgula* for helical, *Thalia cicar* for oblique, *Soestia zonaria* for linear, and *Ritteriella retracta* for bipinnate) and diagrams showing the distinct zooid orientations. The subsequent rows show the frontal view of colonies with four and eight zooids, with the final row indicating the expected frontal area increase factor between the four and the eight zooid colonies. Full black circles in the diagrams represent viscerae while the open circle represent siphons. Black straight lines inside the zooids indicate gill bars while gray straight lines represent endostyles.

The degree of linearity in a colony can be expressed as the degree of parallelism between the zooids and the elongation axis of the colony (Fig. 2). This angle is determined by the degree of developmental dorsoventral zooid rotation, which can span from 90°, in transversal chains with no rotation, to 0° (perfect linearity), in some linear chains such as those from the species *Soestia*

zonaria (Damian-Serrano & Sutherland, 2023). Strong reductions in the dorsoventral zooid rotation angle toward linear forms have evolved multiple times independently (Damian-Serrano et al. 2023), possibly due to adaptive advantages related to their swimming efficiency. Therefore, we further predict that swimming speed is faster in species with lower dorsoventral zooid rotation angle.

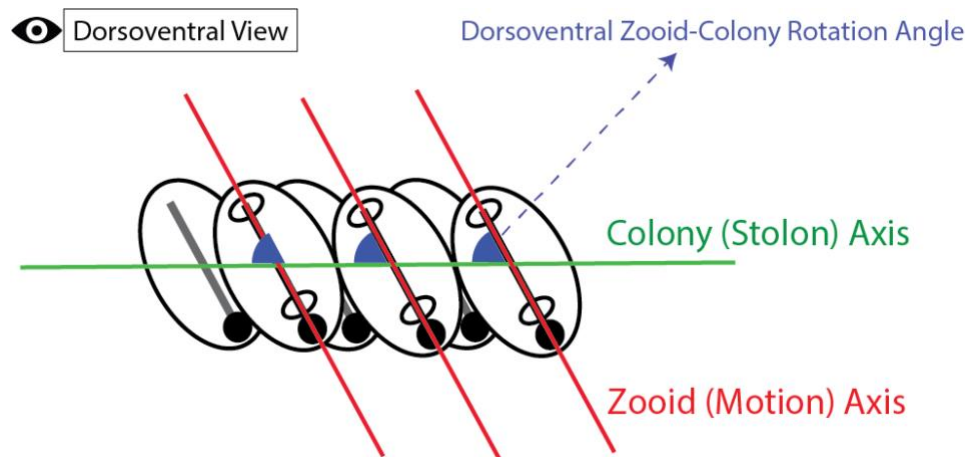


Figure 2. Schematic of an oblique chain from the dorsoventral perspective showing the zooid and stolon axes and the zooid rotation angle (degree of linearity) relative to those axes. Black lines indicate gill bars while gray lines represent endostyles.

Madin (1990) found a linear relationship between swimming effort (pulsation rate) and swimming velocity in solitary zooids and it is reasonable to expect this relationship in colonial zooids. While body size predicts swimming velocity in many animals (Vogel 2008), Madin (1990) did not find such a relationship in salp blastozooids or oozooids. Since asynchronous-pulsating cruising salp colonies overcome many of the acceleration issues that limit single-jetters (Sutherland & Weihs 2017), zooid (propeller) size may also be predictive of swimming speed across species. Salp zooids pump water as a means of filter feeding as well as to move in the water column. The latter function is particularly relevant for species that undergo diel vertical migration, which not all species do (Madin et al. 1996). Therefore, we expect the eco-evolutionary relevance of swimming speed, and the hydrodynamic efficiency may vary between species (Damian-Serrano et al. 2023).

The energetic costs of salp locomotion have been previously estimated using mechanically estimated propulsive efficiency as a proxy in three species (Sutherland & Madin 2010, Gemmell et al. 2021) and with a direct comparison between swimming and anesthetized

respiration rates in *Salpa fusiformis* (Trueman et al. 1984). The metabolic demands of salp colonies have been estimated for a few species of salps in context with other gelatinous zooplankton (Biggs 1977, Schneider 1992, Mayzaud et al. 2005, Trueblood 2019), showing that salps have a relatively higher respiration rate than other gelatinous taxa. Cetta et al. (1986) compared the respiration rates across salp species to their pulsation rate and swimming speeds, revealing that more active species had higher respiration rates. However, the specific costs incurred by their swimming activity and their relationship to swimming speed have never been examined across the diversity of salp species. We expect that species with a higher overall pulsation rate invest more of their metabolic demands in swimming.

In some single-jetters, swimming speed can be directly proportional to the cost of transport (Bi & Zhu 2019) due to a highly inefficient refill phase in the jetting cycle which requires costly acceleration forces to reach high swimming speeds. Since salps are also jet-propelled swimmers, faster-swimming salps may incur higher costs of transport than their slower counterparts.

In this study, we compare the swimming speeds across 17 salp species and the energetic costs of swimming across 15 species, encompassing all six different salp colony architectures (Table S1). In addition, we investigate how swimming speed varies with the number of propeller zooids and evaluate whether differences in frontal area scaling drive disparities between colonial architectures. Finally, we assess how the cost of transport of salp colony swimming varies between species, as well as how it scales with swimming speed and pulsation effort.

Materials and Methods

Fieldwork – We observed salps via bluewater SCUBA diving (Haddock & Heine, 2005) from a small vessel off the coast of Kailua-Kona (Hawai'i Big Island, 19°42'38.7" N 156°06'15.8" W), over 2000 m of offshore water. Some dives were diurnal, where we collected most of the specimens of *Iasis cylindrica*, *Cyclosalpa affinis*, *Cyclosalpa sewelli*, and *Brooksia rostrata*. We observed and collected most specimens of other species during night dives (blackwater diving). We recorded in situ underwater videos of salp colonies swimming using a variety of cameras including primarily a dark field stereovideography system (Sutherland et al. 2024), as well as a lightweight dual GoPro stereo system, a brightfield single-camera system (Colin et al. 2022), and a darkfield single-camera system. The primary stereovideography system was comprised of two synchronized high-resolution cameras (Z Cam E2 and Sync Cable; 4K at 60 or 120 fps) with 17mm f/1.8 lenses (Olympus M.Zuiko Digital) housed in custom aluminum housings (Sexton Company). Each field of view was 23 x 42 mm and in-focus depth was 20-25 mm. The image from the right-hand camera was viewed using an external monitor (Aquatica Digital), and

illumination was provided with two 10,000-lumen lights (Keldan). An L-shaped plastic framer helped the videographer position colonies in the field of view of both cameras. Before diving, the stereo system was calibrated in a swimming pool using a cube with reflective landmarks. Calibration images were processed using the CAL software package (SeaGIS measurement science).

Measuring salp colony swimming speed – For most species, we collected and analyzed footage from multiple specimens (Dataset1A, Table S1). We analyzed the swimming behavior of salp colonies arranged in linear (six species, 64 specimens), bipinnate (three species, 17 specimens), whorl (three species, 10 specimens), cluster (two species, eight specimens), and transversal (one species, two specimens) architectures, with oblique and helical architectures represented by a single specimen. We used a combination of spatially calibrated stereo video and 2D videos with a reference scale in the frame. From the stereo videos, we manually selected and measured the relative XYZ positions of salp colony zooids in EventMeasure (SeaGIS). We implemented a cutoff in the RMS (root mean squared) point error estimate of < 2 mm.

We complemented gaps in taxon sampling with archived 2D videos in the lab from previous expeditions to West Palm Beach (FL, USA) and the Pacific coast of Panama. These two-dimensional single-camera videos were collected using a Sony FDR-AX700 4K Camcorder (3840x2160 pixels, 60-120 fps) with a Gates Underwater Housing using brightfield illumination (Colin et al 2022) or darkfield illumination. For these 2D videos, we used the FFMPEG plugin in ImageJ to manually select and measure the relative XY positions of salp zooids in sequences where the colony was swimming horizontally within the focal plane. The colonies were assumed to be in the same plane as the scale bar so at same distance from the camera. However, in videos with a broad focal depth, this may not always had been the case, thus potentially introducing some measurement error. In addition, when loading the 2D videos in ImageJ, the virtual stack rendered a higher number of frames than those expected from the inherent frame rate. To address this, we calculated an operational frame rate for those videos dividing the number of ImageJ slices by the total duration.

We tracked and manually selected the position of the first zooid's viscera (using a contrast-based centering macro to mark the center point) as well as the position of a reference particle in the water (methods described in Sutherland et al. 2024) in 10-30 frames across 50-500 frame windows spanning 2-4s of swimming on the synchronized left and right videos in EventMeasure. The reference particle was a non-swimming organism (such as a foraminiferan or radiolarian) or a non-living particle. In addition, we recorded the pulsation rates of the specimens measured by counting the number of times the atrial siphon contracted in a known period. For each analyzed

frame, we calculated the horizontal x, vertical y, and depth z (in the case of the stereo video measurement files) components of the relative positions of the frontal zooid to the reference particle as shown in Eq. 1.

$$\begin{aligned} x_n &= x_{n \text{ animal}} - x_{n \text{ particle}} \\ y_n &= y_{n \text{ animal}} - y_{n \text{ particle}} \\ z_n &= z_{n \text{ animal}} - z_{n \text{ particle}} \end{aligned} \quad \text{Eq. 1}$$

Then we calculated the instantaneous relative speeds of the frontal zooid using Eq. 2 (without the z component in the case of the 2D videos) given the known frame rate of each video.

$$U = \frac{\sqrt{(x_2 - x_1)^2 + (y_2 - y_1)^2 + (z_2 - z_1)^2}}{t_2 - t_1} \quad \text{Eq. 2}$$

Salp colonial architecture – To examine the relationships between locomotory variables and colonial architecture, we adopted the species-specific architecture characterizations and dorsoventral zooid rotation angle measurements for each species from Damian-Serrano et al. (2023). Using stills from the underwater videos, we measured zooid length, zooid width, and number of zooids in ImageJ manually selecting the point coordinates. These measurements were repeated in at least three locations from each colony. When a distinct zooid size gradient was observed, we measured zooids in locations from the proximal, middle, and distal regions to capture the full range of variation in the specimen.

Respiration measurements – We collected healthy, adult blastozooid (aggregate stage) colonies across 18 salp species (Dataset S1B) during blue- and black-water SCUBA dives off the coast of Kona (Hawaii, USA) between September 2021 and May 2023. We analyzed the respiration rates of salp colonies arranged in linear (seven species, 46 specimens), bipinnate (three species, 29 specimens), whorl (three species, 23 specimens), cluster (two species, 18 specimens), and transversal (one species, 13 specimens) architectures, oblique chains (*Thalia* sp., seven specimens), and helical architectures represented by *Helicosalpa virgula* (two specimens). Specimens were sealed *in situ* with their surrounding water in plastic jars equipped with a Presens (Germany) oxygen sensor spot and a self-healing rubber port to allow for the injection of solutions without the introduction of air bubbles. We removed as many symbiotic animals from the salps as possible before closing the lid without damaging the colony. The same method was applied to one or more seawater controls to account for the oxygen demand of the

local seawater's microbiome. Several collection events occurred during each 20-60 min long SCUBA dive. Jars with larger animals were opened during the safety stop to allow them to re-oxygenate. Upon the divers' return to the boat, we measured the initial oxygen concentration (mg/l) and temperature, and then repeated the measurements at intervals between 15min and 3h, for total periods ranging between 2h and 5h, depending on logistic constraints in the field and the rate of oxygen depletion. The exact interval time for each measurement was variable but recorded (Dataset S1B).

To estimate the energetic expenditure of different salp species while actively swimming, we recorded the oxygen consumption of intact specimens while swimming inside the jar. To obtain a baseline of basal respiration rate (while not swimming), we anesthetized some specimens before the start of the first oxygen measurement time. A few specimens were used for paired experiments, where their swimming respiration was recorded for a few hours, then inoculated with the anesthetic, and recorded anesthetized for another set of hours. To anesthetize salps, we injected their jars with small volumes of concentrated (50 g/l) bicarbonate-buffered MS-222 through the rubber ports on the lids. We tailored the injection volume to the jar size aiming for a final concentration of 0.2g/l, following the methods in Trueman et al. (1984). We also injected some seawater control jars to evaluate the effect of MS-222 on oxygen concentration in seawater and found no effect.

When multiple seawater controls were collected using jars of different sizes, we paired each jar with the control that had the most similar volume. If among multiple controls only some were jars injected with anesthetic, we paired the anesthetized specimen jars with the injected controls and the intact specimen jars with the intact controls. In experiment 26 (see Dataset S1B for experiment numbers), the control jar was lost due to an encounter with an oceanic white tip shark, thus we paired those measurements with the nearest relative time points from the control jar in experiment 25, collected the same day hours earlier. At the end of each experiment, we identified the salp specimens used in the experiments to the species level, counted the number of zooids, measured the zooid length (total length including projections), and measured the biovolume of the colony using a graduated cylinder. For those specimens where colony or zooid volume was not measured directly, we estimated the colony volume from their zooid length and the number of zooids using a Generalized Additive Model with the measured specimens.

We estimated the oxygen consumption rate for each specimen by fitting a linear regression of consumed oxygen mass (concentration by container volume) against the duration of the measurement series. We subtracted the slope calculated for the relevant control jar to the estimated slope of the animal jar. Since our seawater controls were not filtered, some experiments

had abnormally high estimated background respiration rates, leading to negative values. We removed these data points before the analysis. To estimate biovolume-specific rates, we divided the rates by the colony volumes. We then compared the biovolume-specific respiration rates of active (swimming) and anesthetized specimens within each species, calculating the difference as a measure of biovolume-specific swimming cost respiration rate. We also calculated the relative investment in swimming as the proportion of biovolume-specific respiration rate comprised by the swimming-specific rate. To capture variability within species, we calculated the mean respiration rate of anesthetized specimens for each species and subtracted it from each intact specimen's total respiration rate to get multiple swimming-specific rate values within each species. We noticed that some species had higher average respiration rates among the anesthetized specimens than among the swimming specimens, leading to negative swimming-specific respiration estimates. We interpreted this anomaly as a systematic error due to the extremely low respiration rates of some species that fall within the effective detection limit of our experimental setup given the random variation range of respiration rates in seawater both in experimental jars and in control jars. Small absolute negative values get amplified into large relative values, especially in small animals with a minuscule biovolume denominator. Therefore, we removed the swimming specimens that had lower respiration rates than the mean anesthetized respiration rate for their species. We also removed two respirometry outliers of *Thalia* sp. which had extremely high swimming respiration rates (>7500 pgO₂/ml/min, whereas all other measurements across species including other *Thalia* sp. were limited to 0-1700 pgO₂/ml/min), which were likely due to amplification of experimental error (presence of organic matter or symbionts, underestimation of colony volume due to loss of tiny zooids in the sieves) with the small biovolume denominators in this species.

Estimating costs of transport – We define the cost of transport (COT) as the amount of oxygen consumed per tissue volume per distance traveled by the colony. To estimate the COT, we divided the swimming-specific respiration rates by the mean swimming speed for each species measured from the stereo and 2D video data. Since the specimens used for speed measurements in the videos and those used in the respirometry experiments had different zooid sizes, we used the mean zooid-lengths per second speeds from the video measurements and then multiplied them by the actual zooid lengths of the respirometry specimens to estimate their absolute (mm/s) speeds. Pulsation rate estimates were taken from species averages from the video specimens. We also calculated the size-specific COT by transforming the swimming distances into zooid lengths measured from the respirometry specimens.

Statistical Analyses – All data wrangling and statistics were carried out in R 3.6.3 (R Core Team 2021). To test for differences between architectures, we used ANOVAs with Tukey's post-hoc pairwise contrasts, reporting the difference magnitude and the adjusted p-value in supplementary tables S2A and S2B. To test the relationships between pairs of continuous variables, we used linear models (as well as exponential models when comparing swimming speed to COT) and evaluated the significance of the slope parameter when compared against a flat slope (one-tailed t-test). To evaluate the relative contribution of zooid size, pulsation rate, zooid number, and architecture type on swimming speed, we fitted a generalized linear model and evaluated the significance and proportion of variance explained by each factor using their partial R^2 .

Results

Salp colony swimming speeds, pulsation rates, and respiration rates varied within and across species and colony architectures. Speeds measured with 2D methods were slightly slower than those measured with 3D methods within the species in which they overlapped. This is to be expected since 2D methods cannot account for the z (depth) component of the speed vector. When considering speed in terms of mm/s, we found no relationship between pulsation rate (effort) and absolute speed (Speed mm/s ~ Pulsation rate, adjusted $R^2 = 0.003$, $p = 0.68$, Fig. S1A), but a significant positive relationship with zooid-size corrected speed (Speed zooids/s ~ Pulsation rate, adjusted $R^2 = 0.18$, $p < 0.0001$, Fig. S1B). Moreover, zooid length was positively correlated with speed, whether it is expressed as mm/s (Speed mm/s ~ Zooid length, adjusted $R^2 = 0.06$, $p < 0.0001$, Fig. S1C) or mm/pulse (Speed mm/pulse ~ Zooid length, adjusted $R^2 = 0.42$, $p < 0.0001$, Fig. S1D). Normalized swimming speeds (zooid lengths per pulse) allow for a more direct comparison of swimming speed across colonial architectures.

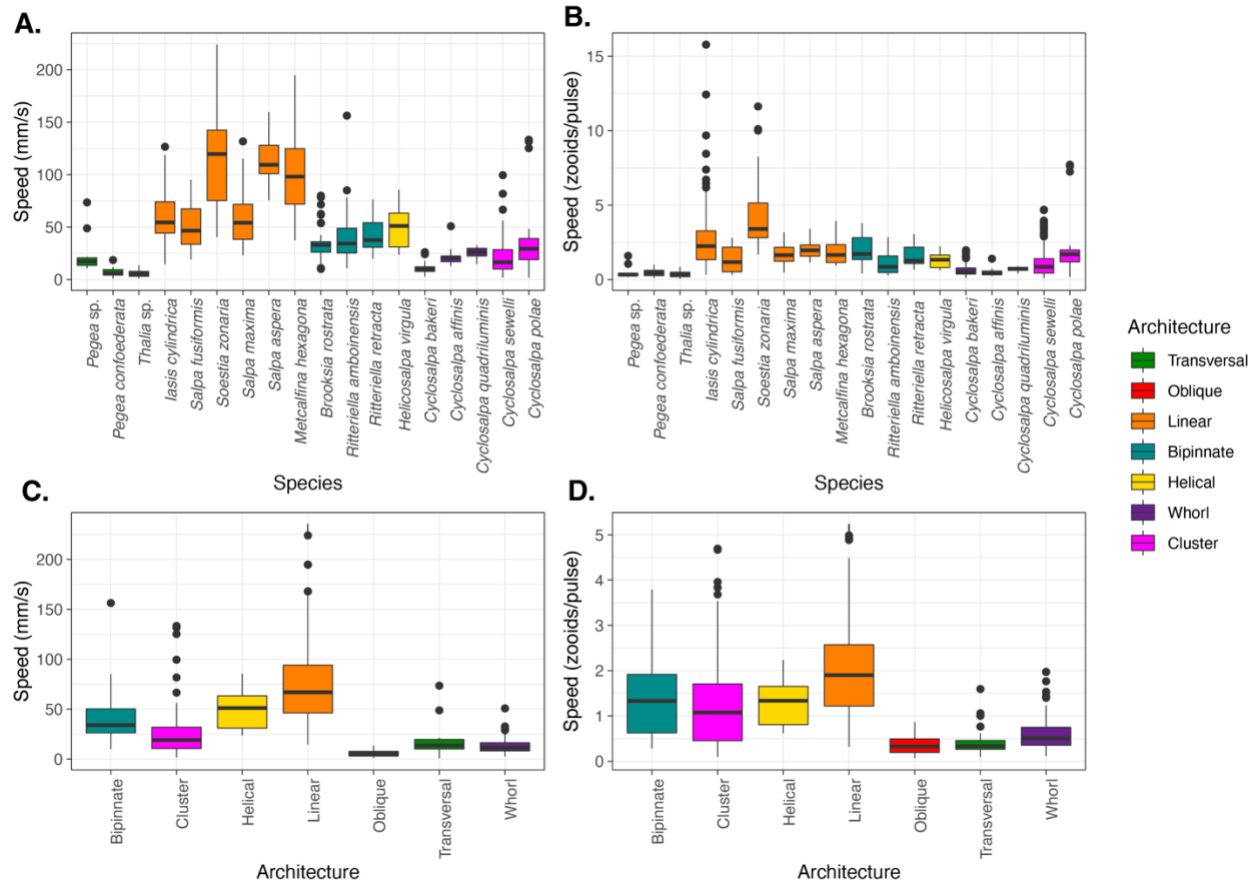


Figure 3. Boxplots showing the absolute (A) and corrected for body size and pulsation rate (B) swimming speeds recorded for each salp species and architecture (C, D) respectively. Colors correspond to colonial architecture types. Sample sizes and Tukey's post-hoc pairwise comparisons across architecture types are listed in Dataset 1A and Table S2A, respectively.

Swimming speed varied significantly (ANOVA $p < 0.001$) between colonial architecture types (Fig. 3C, D, Table S2A). Measurements of helical and oblique chains were limited to a single specimen, so this result should be interpreted with care. In terms of absolute speed (mm/s), linear architectures were significantly faster than every other architecture except helical (Tukey's $p < 0.001$). While bipinnate chains were significantly slower than linear ones and on par to clusters, they were significantly faster than transversal chains, oblique chains, and whorls (Tukey's $p < 0.02$). Clusters were significantly faster than transversal chains, whorls, and oblique chains (Tukey's $p < 0.01$). Transversal chains were on par to whorls and oblique chains, with no significant differences between them.

In terms of relative speed (zoid lengths/pulse), linear architectures were significantly faster than every other architecture except helical (Tukey's $p < 0.001$). Bipinnate chains were

significantly faster than clusters, whorls, transversal chains, and oblique chains (Tukey's $p < 0.008$). Helical chains were significantly faster than whorls and oblique chains (Tukey's $p < 0.03$). Clusters were on par with helical chains for relative speed and were also significantly faster than whorls and oblique chains. Whorls, transversal chains, and oblique chains presented similar relative swimming speeds with no significant differences.

Since linear architectures had faster mean swimming speeds (Fig. 3C, D), we investigated the relationship between swimming speeds with the dorsoventral zooid rotation angle, which represents the degree of linearity of the colony (Fig. 4). Species with more parallel (lower angles) dorsoventral zooid rotation presented faster absolute speeds (Speed mm/s ~ DV Zooid angle, adjusted $R^2 = 0.33$, $p < 0.0001$) and faster size-and-effort corrected swimming speeds (Speed zooids/pulse ~ DV Zooid angle, adjusted $R^2 = 0.09$, $p < 0.0001$).

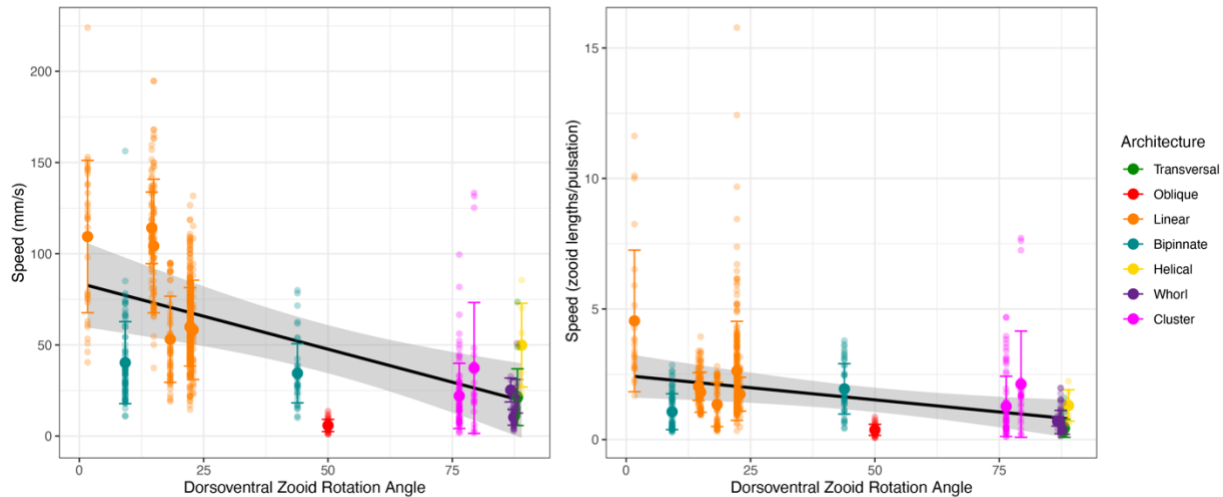


Figure 4. Absolute (A) and relative (B) colony swimming speed (specimen mean with standard errors, total $n=103$) for each salp species across their degree of dorsoventral zooid rotation. Error bars indicate standard error. The color indicates colonial architecture. Gray areas indicate the 95% confidence interval of the linear regression (black line). Species with more parallel (lower angles) dorsoventral zooid rotation present faster absolute speeds (Speed mm/s ~ DV Zooid angle, adjusted $R^2 = 0.33$, $p < 0.0001$) and faster size-and-effort corrected swimming speeds (Speed zooids/pulse ~ DV Zooid angle, adjusted $R^2 = 0.09$, $p < 0.0001$).

We compared how swimming speeds scale with the number of zooids in the colony and found differences between colonial architectures. Swimming speed in whorls increased with number of zooids (Speed mm/s ~ Zooid number, adjusted $R^2 = 0.3$, $p < 0.0001$), though the data

for this architecture was limited to small numbers of zooids (4 to 13) and relatively slow speeds. Linear chain architectures did increase in relative speed with the number of zooids (adjusted $R^2 = 0.14$, $p < 0.001$), as did bipinnate chains (adjusted $R^2 = 0.04$, $p < 0.02$). This relationship was not significant for any of the other architectures.

We pooled the data from multiple architectures into scaling modes to evaluate the overall relationship in colonies with a constant frontal area (linear, bipinnate, and helical species) and in colonies with scaling frontal area (transversal, whorl, cluster, and oblique species) with linear regressions. This aggregation allowed the inclusion of data from architectures for which we only have one specimen (helical and oblique). When pooled by scaling mode (Fig. 5), the regression on colonies with a constant frontal area had a higher intercept on the swimming speed axis than in those with a scaling frontal area (1.54 and 1.09 zooids/pulse, respectively), reflecting the generally higher swimming speed of the former. Moreover, the regression on colonies with constant frontal area had a significant positive slope (Speed mm/s ~ Zooid number, slope = 0.02, adjusted $R^2 = 0.12$, $p < 0.001$), while the regression on those with scaling frontal area was not significant ($p = 0.073$).

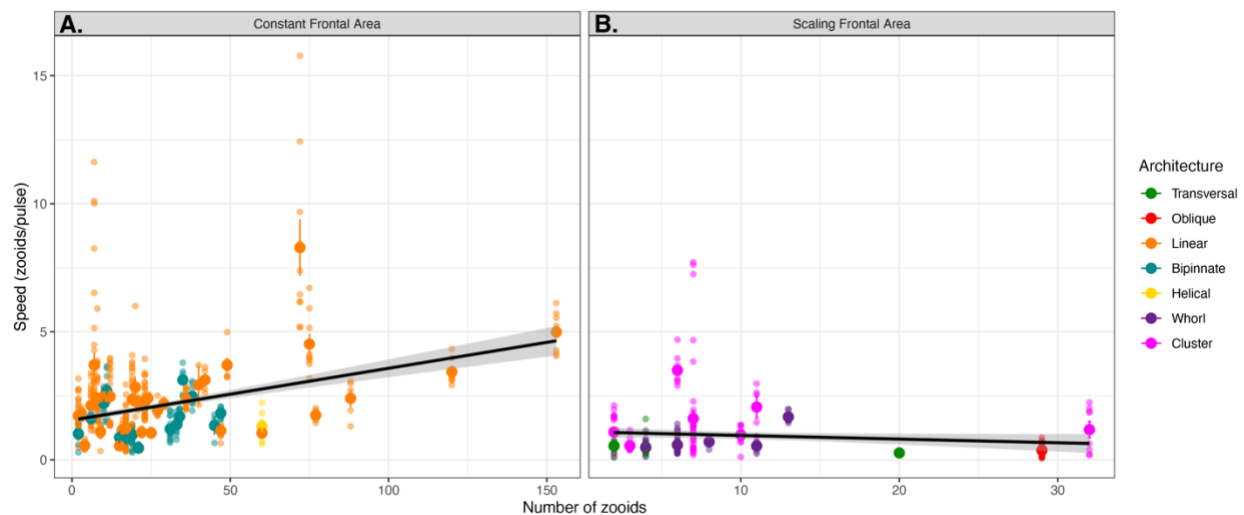


Figure 5. Linear relationships between relative swimming speed (zooid lengths per pulsation, specimen mean with standard errors) and number of zooids in the colony for constant (A) and scaling (n=82) (B) frontal motion-orthogonal frontal area (n=21) scaling modes. Gray areas represent the 95% confidence intervals of the regressions. Colonies with constant frontal area had a significant positive slope (Speed mm/s ~ Zooid number, slope = 0.02, adjusted $R^2 = 0.12$, $p < 0.001$), while the regression on those with scaling frontal area was not significant ($p = 0.073$).

Putting together all the different organismal factors that we analyzed in this study, we calculated a generalized linear regression model to predict absolute salp swimming speed (U) from zooid length (L), pulsation rate (P), number of zooids (N), and colonial architecture represented as frontal area scaling mode (A) as expressed in Eq. 3. While our results suggest that the effect of N depends on A , we favored this simpler regression formula because it had a significantly lower ($\Delta > 70$) AIC score than those with interaction terms between N and A .

$$U \sim L + P + N + A \quad \text{Eq. 3}$$

In this global model, we found significant effects on swimming speed (pseudo- $R^2 = 0.37$, $p < 0.001$) for L , N , and A . We found that our global regression explains 36.76% of the variance in our swimming speed data: 5.78% is explained by zooid size, 3.52% by pulsation rate, 0.81% from zooid number, and 26.64% by the frontal scaling mode.

The respiration rates of swimming and anesthetized salps revealed broad differences between species (Fig. 6, S2A). After estimating COT, we found a few significant differences between architectures (Fig. 6, ANOVA $p < 0.05$, Table S2B). In terms of absolute COT per mm traveled, linear chains, helical chains, bipinnate chains, whorls, and clusters had similar high transport efficiencies under 13 pgO_2/ml . Every one of these architectures was significantly more efficient per mm traveled than oblique architectures (Tukey's $p < 0.001$). In terms of relative COT per zooid length traveled, linear chains and whorls had similar transport efficiencies that are significantly faster than transversal and oblique chains (Tukey's $p < 0.04$). Clusters were also significantly faster than oblique chains (Tukey's $p < 0.01$). Bipinnate and helical chains showed similar values linear chains, clusters, and whorls, but were not significantly more efficient than transversal or oblique chains, perhaps due to insufficient sample sizes. Some of the differences between COT per mm and COT per zooid length are likely due to scaling with body size, as can be observed with the relative shift in the minuscule *Thalia* sp. (5.2 mm zooids) and the massive *Salpa maxima* (93.4 mm zooids).

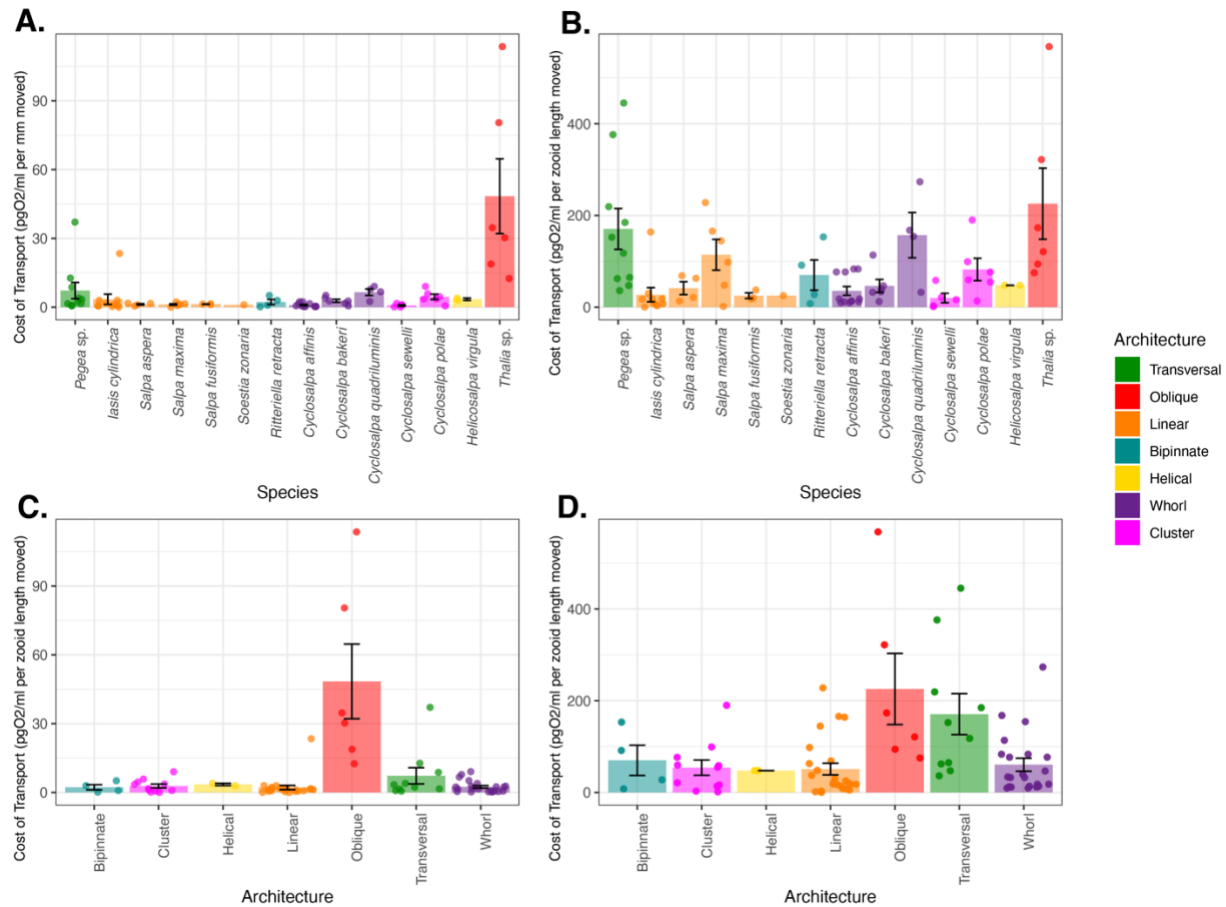


Figure 6. Mean cost-of-transport per mm (A) and per zooid length (B) moved for each salp species, and for each colonial architecture (C, D) with standard errors. Bar colors indicate colonial architecture. Sample sizes and Tukey's post-hoc pairwise comparisons across architecture types are listed in Dataset 1B and Table S2B, respectively.

When comparing the proportion of investment of metabolic costs into swimming (compared to the species mean baseline) across salp species (Fig. S2B), eight species had locomotion budgets under 50%, and the other seven have budgets above 50%.

We then compared the proportion of energetic investment in swimming to the COT values across species (Fig. S3A,B) and found no relationship with absolute COT (Swimming % ~ COT per mm, $p = 0.24$) but found a positive relationship with zooid-length scaled COT (Swimming % ~ COT per zooid length, adjusted $R^2 = 0.22$, $p < 0.001$), indicating that species with more costly locomotion per zooid length invest a larger proportion of their energy budget in swimming. Finally, we compared the proportion of energetic investment in swimming with speed (Swimming % ~ Speed, Fig. S3C,D). We found no relationship (neither in mm/s nor in zooids/s), indicating that faster swimmers do not invest more of their energy budget into their locomotion efforts. We found

that regardless of whether we consider transport in terms of absolute distances (Fig. 7A, linear regression COT per mm ~ Speed mm/s, adjusted $R^2 = 0.09$, $p < 0.005$, exponential regression logCOT per mm ~ Speed mm/s, adjusted $R^2 = 0.14$, $p < 0.001$) or relative to body lengths (Fig. 7B, linear regression COT per zooid length ~ Speed zooids/s, adjusted $R^2 = 0.07$, $p < 0.01$, exponential regression logCOT per zooid length ~ Speed zooids/s, adjusted $R^2 = 0.14$ $p < 0.001$), the COT decreases in species with faster swimming speeds.

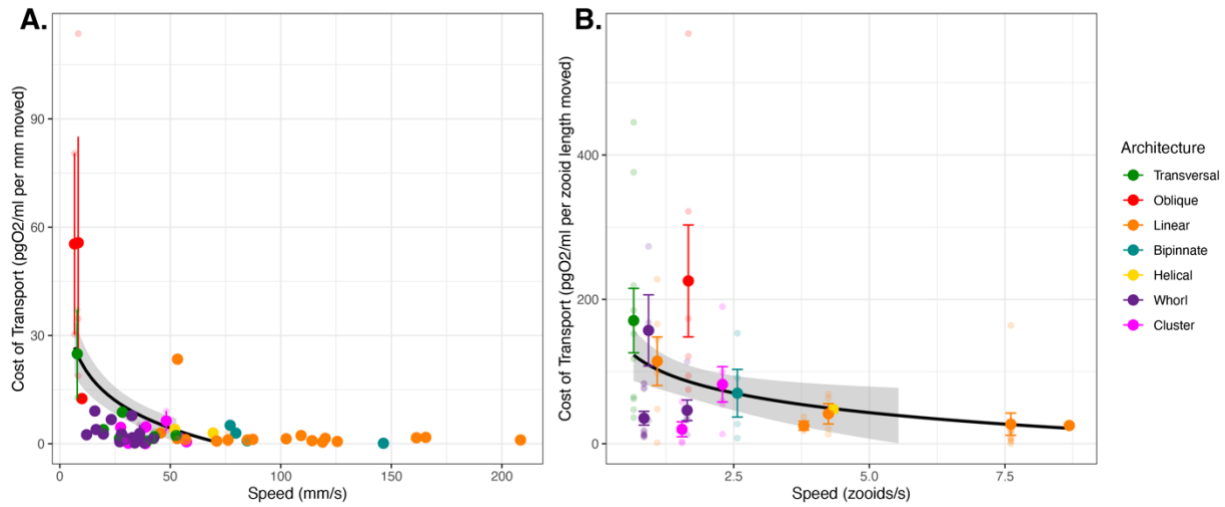


Figure 7. COT (specimen mean with standard error, $n=75$) per mm (A) and zooid length (B) moved across the specimen mean absolute (A) or relative (B) swimming speeds. The dot color indicates colonial architecture. Gray areas represent the 95% confidence intervals of the exponential regressions (black lines). COT decreases in species with faster swimming speeds in terms of absolute distances (exponential regression logCOT per mm ~ Speed mm/s, adjusted $R^2 = 0.14$, $p < 0.001$) and relative to body lengths (exponential regression logCOT per zooid length ~ Speed zooids/s, adjusted $R^2 = 0.14$ $p < 0.001$).

Discussion

We compared the swimming speeds and costs of transport of salp colonies across the most comprehensive representation of salp species diversity. Our results show a wide range of colonial swimming speeds across salp species and architectures. Moreover, this study shows for the first time how salp colonial swimming speed scales with the number of zooids in the colony, suggesting that incremental propulsive power from additional zooids does not always produce higher swimming speeds.

Architectural determinants of salp swimming speed

Colonial architecture was the strongest predictor of swimming speed, though there is a large amount of unexplained variation which may relate to species-specific differences, behavioral, or environmental factors (see global GLM results). We expected that swimming speed in colonial salps would be predicted by pulsation rate as a measure of swimming effort. Our results indicate that this relationship only exists when accounting for zooid size, suggesting an underlying relationship between pulsation rate and zooid size that may be masking its predictive power over absolute speeds. This is consistent with the distribution of our data and our observations in the field where larger salps pulsate at a slower rate than smaller ones. While Madin (1990) found no relationship between zooid size and speed in single zooids, we do find a significant increase in speed with larger zooid sizes, indicating that multi-jet propelled animals follow more similar scaling rules to vertebrate swimmers (Vogel 2008) than to single-jet propellers.

The relationship between the number of zooids and speed in linear chains is complicated by shifts in zooid orientation during development. Salp colonies start their free-living phase when the developing buds detach from the solitary oozoid. This is when the colony is expected to have the maximum number of zooids since the zooid number only gets reduced as the colony splits or loses zooids to turbulence, disease, or predation. Therefore, colonies with higher numbers of zooids are typically composed of smaller, younger zooids. In linear architectures, these younger colonies could still be developing their dorsoventral rotation (Damian-Serrano & Sutherland 2023), thus effectively being more like oblique architecture. A less acute dorsoventral rotation angle would explain why these more numerous linear chains are not as fast as we would expect, given that our results support a significant relationship between this angle and swimming speed (Fig. 4). Finding a strong relationship between zooid number and speed in whorls was surprising given their less hydrodynamic configuration. This could be due to the smaller range of slow speeds and few zooids in the data we obtained for these species. Our regression results on pooled architectures, as well as finding a significant relationship between number of zooids and speed for linear and bipinnate chains but not for clusters nor transversal chains, support our primary hypothesis that the different frontal area scaling relationships across architectures has an impact on swimming speed.

Linear chains swam faster than all other architectures, including those that share a constant frontal area feature like helical and bipinnate chains. One potential explanation for this difference could come from the relative thrust provided by the jets. Linear chains eject their jet plumes at very small angles (near parallel) to the axis of locomotion (Sutherland et al. 2024), just wide enough to avoid interaction between jet plumes (Sutherland & Weihs 2017). Bipinnate and

helical chains (both with constant frontal area) have the atrial siphons (point of jet ejection) of their constituent blastozooids oriented at a wider angle (Madin 1990), which may lead to wider angles of their jets relative to the axis of locomotion. This in turn would result in a larger proportion of the force exerted by the jet to be applied as torque rather than thrust onto the colony. This hypothesis could be tested by measuring the 3D angles of the actual jets instead of the angles of the zooids since salps can use their atrial muscles and siphon morphology to direct the angle of their jets.

Finding that clusters can swim at speeds comparable to those of bipinnate and helical chains, even faster than whorls, defies our intuitive understanding of the mechanical properties of these colonies and thus warrants further investigation into how these species coordinate their jets to produce forward thrust. While oblique chains are architectural intermediates between transversal and linear chains, our data indicates that oblique chains may be the slowest swimmers among salps. This incongruence may be explained by the fact that we only had speed data from one oblique specimen (of *Thalia* sp.) with very small zooid sizes. Small salps might operate at notably lower Reynolds numbers than large ones, which may require a non-linear size correction for meaningful speed comparisons. Swimming speed data from the much larger oblique chains of *Thetys vagina* may provide a more comparable example of the locomotory performance of this oblique colonial configuration.

The questions addressed in this study focus on the effect of frontal area of colonial architectures on swimming speed. This effect may be associated with form and pressure drag differences between more and less streamlined colony shapes. To test whether these are the forces responsible for differences in swimming speed, drag would have to be measured or calculated, which is beyond the scope of this study. Other unaccounted forces may be significant energetic contributors to the system that explain the remainder of the observed variation. Chain length for the streamlined forms (helical, linear, and bipinnate chains) could have negative effects on swimming speeds that may partially counteract the positive effect of increased propeller thrust. For example, skin drag increases proportionally to the surface area of the system, and the smoothness of the chain may increase pressure drag through vortex shredding (Vogel 1981). While added (virtual) mass could also be an issue, asynchronously swimming colonies do not suffer as much from these acceleration-related costs, since their speed is maintained near constant while cruising. Chain length could also lead to reduced stability and efficiency, though some linear species capitalize on this by swimming in corkscrew orbital spirals (Sutherland et al. 2024). However, if friction drag, chain stability, or vortex shredding were indeed more important contributors than frontal form drag, we would predict that linear chains would appear slower than

other more stable and compact architectures. Future studies may unravel these potential confounding effects on the biomechanics of colonial salp swimming.

Salp swimming speed and diel vertical migration

Salps are important players in the oceanic carbon cycle, grazing upon both phytoplankton and bacteria (Henschke et al. 2016). Their carcasses and fecal pellets export large quantities of fixed carbon into the deep sea, accelerating carbon sequestration in the biological carbon pump (Wiebe et al. 1979, Décima et al. 2023). Part of this process is enhanced by the diel vertical migrations by some salp species though the distribution of this behavior across species diversity is poorly known. Off Bermuda, Madin et al. (1996) reported *Pegea* spp., *B. rostrata*, and *C. polae* as non-migratory, all of which we found to have slow swimming speeds. Other slow-swimmer species like *C. affinis* were found to only migrate a few meters through the diel cycle. The species *S. aspera*, *S. fusiformis*, *S. zonaria*, *I. punctata*, and *R. retracta* have been observed vertically migrating off Bermuda (Madin et al 1996, Stone & Steinberg 2014), which is congruent with our observations during fieldwork. These species all have constant frontal area and fast swimming speeds.

Vertical migrators need to be fast enough to follow the dark isolumines as they shift during dawn and dusk in time to maximize their exploitation of the food resources near the surface. Thus, absolute speed is important to the autoecology of these animals. Other *Salpa* species have also been reported as strong vertical migrators throughout the literature (Henschke et al. 2021, Madin et al. 2006, Pascual et al. 2017). A species that does not fit this pattern is *I. cylindrica*, a fast-swimming non-migratory species that spends night and day near the surface (Madin et al 1996; and pers. obs.). However, other studies do report moderate diel vertical migration for this species (Stone & Steinberg 2014), so it may be adapted for facultative vertical migration under specific oceanographic conditions. Some migratory species, such as *S. aspera*, are known to travel distances of over 800m at dawn and dusk, at rates predicted to require 5-10 m/min (83-166 mm/s) based on MOCNESS trawl intervals (Wiebe et al. 1979). These predictions are consistent with the speeds we recorded for this species (88-145 mm/s) and similar congeners.

Ecophysiological implications

While the importance of a few well-studied linear chain salp species in the biological carbon pump has been delineated, the question of whether this ecological role is generalizable to other salp species remains unanswered. In addition to vertical migration behavior, another likely important factor in their carbon flow is their respiration rate. The higher their respiration rate, the larger the proportion of assimilated carbon that will be released back into the water as dissolved carbon dioxide. This study provides the broadest taxonomic perspective on respiration rates (18

species, Fig. S2A) and swimming cost of transport (14 species), finding 17-fold differences in their respiration rates and over 77-fold differences in their mean COT. Except for a few species with extremely high and low values, most respiration rates are centered between 0.2 and 1 $\mu\text{mol/g/hour}$, assuming a salp tissue density of 1.025 g/ml. In general, the respiration rates we estimated for salps are within the range of those reported in the literature (Trueblood 2019, Iguchi and Ikeda 2004). Compared to the metabolic rates estimated for the broader diversity of marine pelagic animals (Seibel & Drazen 2007), the rates that we measured for salps are in a similar range to those measured for *Salpa thompsoni* (Iguchi and Ikeda 2004). Our values are also similar to those measured by Seibel & Drazen (2007) in nemerteans, chaetognaths, and most fishes (0.1-1 $\mu\text{molO}_2/\text{g/h}$), which are generally higher than other gelatinous animals like ctenophores or scyphomedusae (0.01-0.1 $\mu\text{molO}_2/\text{g/h}$), but generally lower than those of cephalopods, crustaceans, or large fish (1-10 $\mu\text{molO}_2/\text{g/h}$). Salp species known to have strong vertical migration behaviors (*Salpa* spp., *S. zonaria*, *I. punctata*, and *R. retracta*) have low basal metabolic rates (Fig. S2A) and low costs of transport. These results indicate that many non-migratory species, while likely still being important players in the biological carbon pump via their fecal pellet production, are releasing more of the consumed carbon as carbon dioxide near the surface than their more metabolically efficient relatives. The ultimate ecological outcome of each species needs to be assessed holistically, considering their microbial filtration and pellet deposition rate as well as their relative abundance in the water column.

Our metabolically calculated costs of transport range between 5-50 J/kg/m when converting the mg of oxygen to J via aerobic respiration free energy equations at 23°C. Our values are higher than the highly efficient 1-2 J/kg/m reported for salps in the literature (Bone & Trueman 1983, Gemmell et al. 2021), rather approaching the less-efficient values found in single jet-propelled invertebrates like scallops or squids. We suspect that COT calculated from mechanical parameters such as the displacement of water mass is not directly comparable to the COT calculated from respiration rates. Furthermore, the standard aerobic respiration free-energy equation based on glucose may not fully represent the metabolic energy-conversion processes in salps, which may rely on a combination of sugars and fatty acids derived from their microscopic prey.

While other studies on jet-propelled systems have shown that COT increases with swimming speed (Bi & Zhu 2019), we did not find support for this hypothesis. This may be due to salps being unique among jet-propelled animals since their incurrent flow is separate, parallel, and thus synergistic with the excurrent flow on the opposite end of their bodies, avoiding the deceleration forces typically associated with the refill phase (Bone and Trueman, 1983). Our

results show that faster swimming species have lower COT (Fig. 6), which suggests that faster speeds and higher locomotory efficiency have a common cause, where both speed and efficiency depend on frontal area which may partly drive form and pressure drag forces. However, this hypothesis is not supported by the distribution of COT across architectures (Fig 6C, D), where except for oblique and transversal chains, all architectures present similarly efficient COT values. Perhaps there are other underlying explanatory factors linking swimming speed and swimming efficiency, such as shared ancestry, muscle content, jet coordination, or jetting angles (thrust-to-torque ratios).

Evolutionary implications

Across the evolutionary history of salps, linear chains have evolved multiple times independently from oblique ancestors (Damian-Serrano et al. 2023), suggesting the adaptive role of this architecture as a functional trait. Linear chain architectures evolved independently in *M. hexagona*, *S. zonaria*, *I. punctata*, and before the common ancestor of *Iasis* and *Salpa*. Our results show that going from an oblique form to a linear one may confer significant advantages in locomotory speed and energetic efficiency. However, multiple colonial architectures, which we find to be slower swimmers (such as transversal chains, helical chains, whorls, and clusters in the genus *Pegea* and the Cyclosalpidae family) had also evolved from oblique and linear ancestors. This is incongruent with a scenario where natural selection strongly favors locomotion efficiency across all ecological niches of salps. Therefore, the evolution of colonial architecture may be driven by ecological trade-offs with other non-locomotory functions. Alternatively, in some of these lineages, locomotion at the colonial stage may not be important enough for selection to maintain these highly hydrodynamic forms, allowing for neutral evolutionary processes to produce a diversity of non-adaptive forms. We do not expect the relationships between speed, architecture, and energetic efficiency to be a result of them co-evolving with one another, but rather a result of present mechanical relationships derived from colonial form. Therefore, it would not be appropriate to analyze these relationships using phylogenetic comparative methods. However, there may be unaccounted factors explaining the residual variation in our analyses that may bear phylogenetic signal. For example, tunic stiffness, tunic smoothness, muscle band number, muscle fiber density, swimming behavior, as well as metabolic and physiological baselines may be more similar between more closely related species, potentially erasing some of the architecture-specific signal. Future studies may address the role of phylogeny and heritable factors in salp swimming speed and cost of transport. These factors may have co-evolved with each other and/or with respiration rate or colonial architecture.

Insights for bioinspired underwater vehicle design

Pulsatile jet propulsion is a promising avenue for bioinspired aquatic vehicles and robots (Mohensi 2006, Gohardini 2014, Yue et al. 2015). Multijet propulsion systems with multiple propellers akin to salp colonies have been explored in an engineering context (Chao et al. 2017, Costello et al. 2015) with direct inspiration from gelatinous animals (Marut 2014, Krummel 2019, Bi et al 2022, Du Clos et al. 2022). Salp diversity provides a natural laboratory to explore the hydrodynamic implications of different multijet arrangement designs. Our findings underscore the importance of considering the scaling hydrodynamic properties of propeller arrangements to optimize speed and energy efficiency in bioinspired underwater vehicle design. While linear chain arrangements were the fastest and among the most energy efficient, robot (or vehicle) configurations such as a cluster form may confer unique object manipulation or maneuverability advantages. Our results show that these seemingly inefficient propeller configurations do not impose large disadvantages in terms of speed and fuel efficiency.

Acknowledgments:

We are grateful to the crew of Aquatic Life Divers, Kona Honu Divers for their assistance and support in hosting our offshore diving operations. We also wish to thank Marc Hughes, Jeff Milisen, Rebecca Gordon, Matt Connelly, Clint Collins, Paul Richardson, and Anne Thompson for their assistance during diving, collections, and filming operations in the field. Finally, we would like to thank Tiffany Bachtel for her valuable advice on the respirometry experiment design.

Funding

This research was supported by the Gordon and Betty Moore Foundation [grant number 8835] and the Office of Naval Research [grant number N00014-23-1-2171].

Data availability

Data used to generate the results presented in this paper are available in the supplementary information. Any other datasets used directly or indirectly for this study are available from the authors upon reasonable request.

Competing interests

No competing interests declared.

Literature cited

- Alexander, A. J. (1968). Forward Speed Effects on Annular Jet Cushions. The Aeronautical Journal, 72(689), 438-441.
- Bi, X., & Zhu, Q. (2019). Dynamics of a squid-inspired swimmer in free swimming. Bioinspiration & Biomimetics, 15(1), 016005.
- Bi, X., Tang, H., & Zhu, Q., 2022. Feasibility of hydrodynamically activated valves for 416 salp-like propulsion. Physics of Fluids, 34(10), 101903.

677 Biggs, D. C. (1977). Respiration and ammonium excretion by open ocean gelatinous zooplankton
678 1. *Limnology and Oceanography*, 22(1), 108-117.

679 Bone, Q., Anderson, P. A. V., & Pulsford, A. (1980). Morphology of salp chain communication.
680 *Proceedings of the Royal Society of London. Series B. Biological Sciences*, 210(1181),
681 549-558.

682 Bone, Q., & Trueman, E. R. (1983). Jet propulsion in salps (Tunicata: Thaliacea). *Journal of*
683 *Zoology*, 201(4), 481-506.

684 Cetta, C. M., Madin, L. P., & Kremer, P. (1986). Respiration and excretion by oceanic salps.
685 *Marine Biology*, 91, 529-537.

686 Chao, S., Guan, G., & Hong, G. S., 2017, September. Design of a finless torpedo-shaped micro
687 AUV with high maneuverability. In *OCEANS 2017-Anchorage* (pp. 425 1-6). IEEE.

688 Colin, S. P., Gemmell, B. J., Costello, J. H., & Sutherland, K. R. (2022). In situ high-speed
689 brightfield imaging for studies of aquatic organisms. *Protocols.io*.

690 Costello, J. H., Colin, S. P., Gemmell, B. J., Dabiri, J. O., & Sutherland, K. R., 2015. 429 Multi-jet
691 propulsion organized by clonal development in a colonial siphonophore. 430 *Nature*
692 *communications*, 6(1), 8158.

693 Damian-Serrano, A., & Sutherland, K. R. (2023). A developmental ontology for the colonial
694 architecture of salps. *The Biological Bulletin*, 245(1), 9-18..

695 Damian-Serrano, A., Hughes, M., & Sutherland, K. R. (2023). A new molecular phylogeny of salps
696 (Tunicata: thaliacea: salpida) and the evolutionary history of their colonial architecture.
697 *Integrative Organismal Biology*, 5(1), obad037.

698 Décima, M., Stukel, M. R., Nodder, S. D., Gutiérrez-Rodríguez, A., Selph, K. E., Dos Santos, A.
699 L., ... & Pinkerton, M. (2023). Salp blooms drive strong increases in passive carbon export
700 in the Southern Ocean. *Nature communications*, 14(1), 425.

701 Du Clos, K. T., Gemmell, B. J., Colin, S. P., Costello, J. H., Dabiri, J. O., and Sutherland, K. R.
702 2022. Distributed propulsion enables fast and efficient swimming modes in physonect
703 siphonophores. *Proceedings of the National Academy of Sciences*. 119:e2202494119.

704 Gemmell, B. J., Dabiri, J. O., Colin, S. P., Costello, J. H., Townsend, J. P., & Sutherland, K. R.
705 (2021). Cool your jets: biological jet propulsion in marine invertebrates. *Journal of*
706 *Experimental Biology*, 224(12), jeb222083.

707 Gohardani, A. S. *Distributed Propulsion Technology* Nova Science Publishers (2014).

708 Haddock, S. H. (2004). A golden age of gelata: past and future research on planktonic
709 ctenophores and cnidarians. *Hydrobiologia*, 530, 549-556.

710 Haddock, S. H., & Heine, J. N. (2005). Scientific blue-water diving.

711 Hamner, W. M., Madin, L. P., Alldredge, A. L., Gilmer, R. W., & Hamner, P. P. (1975). Underwater
712 observations of gelatinous zooplankton: Sampling problems, feeding biology, and
713 behavior 1. *Limnology and Oceanography*, 20(6), 907-917.

714 Henschke, N., Cherel, Y., Cotté, C., Espinasse, B., Hunt, B.P. and Pakhomov, E.A., 2021. Size
715 and stage specific patterns in *Salpa thompsoni* vertical migration. *Journal of Marine*
716 *Systems*, 222, p.103587.

717 Krummel, G. M. (2019). Locomotion and Control of Cnidarian-Inspired Robots (Doctoral
718 dissertation, Virginia Tech).

719 Mackie, G. O. (1986). From aggregates to integrates: physiological aspects of modularity in
720 colonial animals. *Philosophical Transactions of the Royal Society of London. B, Biological*
721 *Sciences*, 313(1159), 175-196.

722 Madin, L. P. (1990). Aspects of jet propulsion in salps. *Canadian Journal of Zoology*, 68(4), 765-
723 777.

724 Madin, L. P., & Deibel, D. (1998). Feeding and energetics of Thaliacea. *The biology of pelagic*
725 *tunicates*, 81-104.

726 Madin, L. P., Kremer, P., & Hacker, S. (1996). Distribution and vertical migration of salps
727 (Tunicata, Thaliacea) near Bermuda. *Journal of Plankton Research*, 18(5), 747-755.

728 Madin, L.P., Kremer, P., Wiebe, P.H., Purcell, J.E., Horgan, E.H. and Nemazie, D.A., 2006.
729 Periodic swarms of the salp *Salpa aspera* in the Slope Water off the NE United States:
730 Biovolume, vertical migration, grazing, and vertical flux. *Deep Sea Research Part I:*
731 *Oceanographic Research Papers*, 53(5), pp.804-819.

732 Marut, K. J. (2014). Underwater Robotic Propulsors Inspired by Jetting Jellyfish (Doctoral
733 dissertation, Virginia Tech).

734 Mayzaud, P., Boutoute, M., Gasparini, S., Mousseau, L., & Lefevre, D. (2005). Respiration in
735 marine zooplankton—the other side of the coin: CO₂ production. *Limnology and*
736 *Oceanography*, 50(1), 291-298.

737 Mohensi, K., 2006. Pulsatile vortex generators for low-speed maneuvering of small 482
738 underwater vehicles. *Ocean Eng.* 33, 2209–2223.

739 Pascual, M., Acuña, J.L., Sabatés, A., Raya, V. and Fuentes, V., 2017. Contrasting diel vertical
740 migration patterns in *Salpa fusiformis* populations. *Journal of Plankton Research*, 39(5),
741 pp.836-842.

742 R Core Team, R. (2021). R: A language and environment for statistical computing.

- Schneider, G. (1992). A comparison of carbon-specific respiration rates in gelatinous and non-gelatinous zooplankton: a search for general rules in zooplankton metabolism. *Helgoländer Meeresuntersuchungen*, 46, 377-388.
- Seibel, B. A., & Drazen, J. C. (2007). The rate of metabolism in marine animals: environmental constraints, ecological demands and energetic opportunities. *Philosophical Transactions of the Royal Society B: Biological Sciences*, 362(1487), 2061-2078.
- Stone, J. P., & Steinberg, D. K. (2014). Long-term time-series study of salp population dynamics in the Sargasso Sea. *Marine Ecology Progress Series*, 510, 111-127.
- Sutherland, K. R., & Weihs, D. (2017). Hydrodynamic advantages of swimming by salp chains. *Journal of The Royal Society Interface*, 14(133), 20170298.
- Sutherland, K. R., Damian-Serrano, A., Du Clos, K. T., Gemmell, B. J., Colin, S. P., Costello, J. H. (2024). Spinning and corkscrewing of oceanic macroplankton revealed through in situ imaging. *Science Advances* 10(20).
- Sutherland, K. R., & Madin, L. P. (2010). Comparative jet wake structure and swimming performance of salps. *Journal of Experimental Biology*, 213(17), 2967-2975.
- Trueblood, L. A. (2019). Salp metabolism: temperature and oxygen partial pressure effect on the physiology of *Salpa fusiformis* from the California Current. *Journal of Plankton Research*, 41(3), 281-291.
- Trueman, E. R., Bone, Q., & Braconnot, J. C. (1984). Oxygen consumption in swimming salps (Tunicata: Thaliacea). *Journal of Experimental Biology*, 110(1), 323-327.
- Vogel, S. (1981). Life in moving fluids. *Princeton University Press*, Princeton, NJ.
- Vogel, S. (2008). Modes and scaling in aquatic locomotion. *Integrative and Comparative Biology*, 48(6), 702-712.
- Wiebe, P. H., Madin, L. P., Haury, L. R., Harbison, G. R., & Philbin, L. M. (1979). Diel vertical migration by *Salpa aspera* and its potential for large-scale particulate organic matter transport to the deep-sea. *Marine Biology*, 53, 249-255.
- World Register of Marine Species (WoRMS). (2024). WoRMS Editorial Board. Accessed January 30, 2024. Available online at <http://www.marinespecies.org>
- Yue, C. et al., 2015. Mechantronic system and experiments of a spherical underwater 510 robot: SUR-II. *J. Intell. Robot Syst.* Doi:10.1007/s10846-015-0177-3.